Laboratory Investigation (2013) 93, 1219–1231

All-transretinoic acid ameliorates bleomycin-induced lung fibrosis by downregulating the TGF-β1/Smad3 signaling pathway in rats

Xiaodong Song[1,5], Weili Liu[2,5], Shuyang Xie[3], Meirong Wang[1,4], Guohong Cao[1,2], Cuiping Mao[1] and Changjun Lv[1,2]

The transforming growth factor-β1 (TGF-β1)/Smad3 signaling pathway has a central role in pathogenesis of lung fibrosis. In the present study, we investigated if all-trans retinoic acid (ATRA) could attenuate fibrosis in bleomycin (BLM)-induced lung fibrosis in rats through regulating TGF-β1/Smad3 signaling. Beginning on day 14 after BLM administration, the ATRA I and II groups of rats received daily oral administration of ATRA for 14 days. All rats were killed on day 28. Lung tissue sections were prepared and subject to histological assessment, and expression levels of proteins involved in the TGF-β1 signaling cascade and epithelial–mesenchymal transition (EMT) were evaluated by transmission electron microscopy (TEM), quantitative real-time polymerase chain reaction (qRT-PCR), western blot procedure, and immunohistochemical or immunofluorescence staining. BLM significantly increased the alveolar septum infiltrates, inflammatory cell infiltrates, and collagen fibers. These BLM-induced changes were significantly ameliorated by ATRA treatment. In addition, BLM significantly increased levels of lung fibrosis markers α-SMA, hydroxyproline (Hyp), collagen I, Snail, and Twist, whereas significantly decreased E-cadherin expression. ATRA treatment largely reversed BLM-induced changes in these lung fibrosis markers. ATRA also blocked BLM-induced activation of the TGF-β1/Smad3 signaling pathway in lung tissues, including expression of TGF-β1, Smad3, p-Smad3, zinc-finger E-box-binding homeobox 1 and 2 (ZEB1 and ZEB2), and the high-mobility group AT-hook 2 (HMGA2). Our results suggest that ATRA may have potential therapeutic value for lung fibrosis treatment.

Laboratory Investigation (2013) **93,** 1219–1231; doi:10.1038/labinvest.2013.108; published online 16 September 2013

KEYWORDS: all-transretinoic acid; collagen; lung fibrosis; Smad3; TGF-β1

Lung fibrosis is an aggressive disease with a median survival of 3–5 years after the onset of symptoms. It involves replacement of normal lung parenchyma with fibrotic tissue accompanied by inflammation, fibroblast proliferation, and excessive collagen deposition. The scar tissue once formed is permanent, leading to irreversible decrease in oxygen-diffusion capacity of the lung. Lung fibrosis may be a secondary effect of other diseases or conditions, or appear without any known cause, in which it is called 'idiopathic'. The cellular and molecular mechanisms underlying pathogenesis of lung fibrosis are largely unclear. To date, there is no evidence that any medications can prevent or reverse lung fibrogenesis, and new therapies are urgently needed for effective treatment.[1] Pharmaceutical interventions of factors involved in fibroblast proliferation, inflammation, oxidative damage, and extracellular matrix formation have been intensively explored as potential new therapies. The transforming growth factor-β1 (TGF-β1)/Smad3 signaling pathway has a central role among various factors that regulate lung fibrosis. TGF-β1 induces differentiation of lung fibroblasts into myofibroblasts characterized by expression of α-smooth muscle actin (α-SMA) and synthesis of extracellular matrix proteins.[2–4] Downstream signaling effects of TGF-β1 are mediated by Smad3,[5] and Smad3 deficiency attenuates bleomycin (BLM)-induced lung fibrosis.[6] Inhibition of TGF-β1/Smad3 signaling with a variety of biologics including neutralizing antibodies, antisense oligonucleotides, and short-interfering RNAs

[1]Medicine Research Center, Binzhou Medical University, Yantai, China; [2]Department of Respiratory Medicine, Affiliated Hospital to Binzhou Medical University, Binzhou, China; [3]Department of Biochemistry and Molecular Biology, Binzhou Medical University, Yantai, China and [4]Clinical laboratory, Affiliated Hospital to Binzhou Medical University, Yantai, China

Correspondence: Professor C Lv, MD, PhD, Medicine Research Center of Binzhou Medical University, No. 346, Guanhai Road, Laishan District, Yantai 264003, China. E-mail: luky_lcj@126.com

[5]These authors contributed equally to this work.

Received 27 March 2013; revised 11 August 2013; accepted 14 August 2013

(siRNAs) has been reported to ameliorate fibrosis, validating the TGF-β1/Smad3 pathway as a therapeutic target for the treatment of lung fibrosis.[7–9] However, biologics drugs are difficult to develop owing to factors such as their poor stability and bioavailability. For example, canonical double-stranded siRNAs are unstable and cause undesirable adverse effects such as deregulation of the immune system. Their therapeutic value is also limited by potential oncogenic effect of the vectors. Thus, RNAi-based therapy is already clinically applied; however, recommending this therapy to every patient remains difficult.[10]

All-trans retinoic acid (ATRA), a derivative of vitamin A, exhibits a number of beneficial effects such as anti-proliferative, anti-inflammatory, anti-migratory, and anti-fibrogenic activities. ATRA is currently used to induce remission in patients with acute promyelocytic leukemia and has the potential to be used to treat solid tumors.[11,12] Several studies have demonstrated the anti-fibrogenic effect of ATRA in BLM-induced lung fibrosis in mice.[13,14] However, Segel *et al*[15] reported that ATRA does not elicit beneficial effects on BLM-induced lung fibrosis in rats. Although there is controversy in the effect of ATRA on lung fibrogenesis in animal models, the effect of ATRA on the TGF-β1/Smad3 pathway in lung fibrosis has not been reported. A recent paper showed that ATRA suppresses kidney fibrosis without suppressing the TGF-β1/Smad3 signaling in rat.[16] Zhou *et al*[17] proposed that these divergent and contradictory effects may be because of the different signaling transduction pathways involved in various tissues and/or cells. The different ATRA doses used in various studies may be another reason for the contradictory results. In the present study, we aimed to determine whether ATRA (0.4 and 1.6 mg/kg) can ameliorate BLM-induced lung fibrosis in rats and whether the mechanism involves the downregulation of the TGF-β1/Smad3 signaling pathway.

MATERIALS AND METHODS

Ethics Statement

Sprague–Dawley (SD) rats with a mean weight of 200 g were provided by the Green Leaf Experimental Animal Center (Yantai, China). All animal experiments were performed in accordance with the regulations established by the Committee on the Ethics of Animal Experiments of Binzhou Medical University. The rats were housed under a 12-h light/dark cycle and were allowed free access to food and water.

Animal Model

Pharmaceutical grade BLM was purchased from Nippon Kayaku (Tokyo, Japan). ATRA was purchased from Sigma (St Louis, MO, USA). The lung fibrosis model was established as previously described.[18] A total of 40 SD rats were randomly divided into four groups (10 rats each) including the sham group, BLM-induced group (BLM group), ATRA treatment I group (ATRA I group, 0.4 mg/kg), and ATRA treatment II group (ATRA II group, 1.6 mg/kg).[19] Lung fibrosis was induced by a single intratracheal instillation of 5 mg/kg BLM in 0.3 ml of saline in all the groups except the sham group. The sham group received an equal volume of saline. Beginning on day 14 after BLM treatment, rats in ATRA I and II groups received oral ATRA once daily for 14 days. On day 28, all rats were killed, and lung tissue sections were collected and immediately frozen in liquid nitrogen for further studies.

Hematoxylin and Eosin (H&E) Staining

H&E staining agents were purchased from Sigma. Lung tissues were fixed by instilling 4% paraformaldehyde through the trachea and were embedded in paraffin. Transverse sections of 4 μm thickness were stained with H&E following the manufacturer's standard protocol. Histologic grading of lesions was performed using the Szapiel method for extent of inflammation in lung parenchyma base.[20] Degrees of microscopic interstitial inflammation and fibrosis were graded on a scale of 1–4. (1), absent and appears normal ($-$); (2), light ($+$); (3), moderate ($++$); (4), strong ($++++$). In addition, total lung inflammation and fibrosis score were calculated as the sum of the two components. Three sections collected from each lung were analyzed in the experiment.

Masson's Trichrome Staining

Collagen deposition was measured by the Masson's trichrome method. Lung tissues were fixed by inflation with 4% paraformaldehyde overnight, dehydrated in 70% ethanol, and embedded in paraffin wax. Sections of 4 μm thickness were prepared and stained with Masson's trichrome. Percentage of fibrosis in the lung was determined by counting the number of pixels within areas of stained collagen in digital images, using the Adobe Photoshop CS3 program as previously described.[21] We can calculate the hydroxyproline (Hyp) content according to the depth of coloration using the following formula: Hyp content (μg/mg wet weight) = (measurement tube absorbance $-$ absorbance of blank)/standard pipe of absorbance $\times$ content of standard pipe $\times$ total volume of hydrolyzate/tissue wet weight. Degrees of microscopic interstitial inflammation and fibrosis were graded on a scale of 1–4. (1), absent and appears normal ($-$); (2), light ($+$, affected area $<20\%$); (3), moderate ($++$, affected area 20–40%); (4), strong ($++++$, affected area $>50\%$). Three sections collected from each lung were analyzed in the experiment.

Immunohistochemistry

Anti-collagen I antibody was purchased from Santa Cruz Biotechnology (Dallas, TX, USA). Paraffin sections prepared as described above were dewaxed and immersed in 3% hydrogen peroxide solution in methanol for 10 min to block endogenous peroxidases. The slides were subsequently immersed in 10 mM citrate buffer (pH 6.0) and placed in a microwave oven for 25 min. After washing with 10 mM

phosphate-buffered saline (PBS; pH 7.4), the sections were covered with serum and placed in a humidity chamber for 30 min at room temperature. Excess serum was rinsed off with 10 mM PBS, and the sections were incubated with anti-collagen I antibody (1:500) in a humidity chamber for 45 min at room temperature. The sections were then rinsed with PBS and incubated with biotinylated secondary antibody in a humidity chamber for 40 min at 37 °C. After rinsing with PBS, the slides were incubated with streptavidin–peroxidase complex reagent for 45 min at room temperature and washed again with PBS. The slides were covered with 3,3-diaminobenzidine tetrahydrochloride solution for 15 min and then examined under a microscope. The sections were then immersed in running water, counterstained with haematoxylin for 1 min, and immersed in tap water bath followed by a series of alcohol baths of increasing concentrations and xylene. The processed sections were covered with cover slips. Samples treated with primary antibody alone were assigned as negative controls.

Transmission Electron Microscopy (TEM) Observation

Lung tissues were fixed by treatment with fresh 3% glutaraldehyde at 4 °C for at least 4 h, postfixed in 1% osmium tetroxide for 1.5 h, dehydrated in gradient ethanol, infiltrated with Epon812, embedded, and cultured at 37, 45, and 60 °C for 24 h. Ultrathin sections prepared with an ultracut E ultramicrotome were stained with uranyl acetate and lead citrate and observed using a JEM-1400 TEM system from Jeol (Tokyo, Japan).[22]

Hyp Content

Lung specimens were washed with saline and hydrolyzed with 0.6% hydrochloric acid at 100 °C for 5 h. The hydrolysates were neutralized with sodium hydroxide and diluted with distilled water. Hyp level in the hydrolysates was colorimetrically determined by absorbance at 560 nm with p-dimethylaminobenzaldehyde and expressed as mg/g wet tissue.[23]

Immunofluorescence

Rabbit anti-rat α-SMA and anti-E-cadherin antibodies were purchased from Boster Bio-engineering (Wuhan city, China). Immunofluorescence staining was performed as previously described.[18] Lung tissue sections were fixed in 4% paraformaldehyde, rinsed with PBS solution, incubated with 0.5% TritonX-100 for 20 min, and blocked with 10% calf serum. Tissue sections were incubated with rabbit anti-rat α-SMA or E-cadherin antibody (1:100 or 1:50) at 4 °C overnight. Tissue sections were subsequently rinsed with PBS and incubated with goat anti-rabbit IgG labeled with FITC or Cy3. Hoechst 33258 fluorochrome (Sigma) was used for nuclear staining. After washing with PBS, tissue sections were mounted in neutral glycerin and analyzed under a laser scanning confocal microscope from Leica Company (Germany). The fluorescence imaging was conducted with excitation at 488 nm and emission at 510 nm at room temperature.

Quantitative Real-time Polymerase Chain Reaction (qRT-PCR)

Total RNA was extracted from lung tissues using TRIzol reagent from Invitrogen (Carlsbad, CA, USA) according to the manufacturer's instructions. Complementary DNA synthesis was performed using the M-MLV reverse transcriptase kit from Promega (Madison, WI, USA) following the manufacturer's instructions. qRT-PCR was performed using a SYBR green-based PCR master mix kit from Takara Bio (Shiga, Japan) on a Rotor Gene3000 real-time PCR system from Corbett Research (Sydney, Australia). The PCR conditions were as follows: initial denaturation at 95° C for 5 min followed by 40 cycles of 60 °C for 25 s, annealing at 52 °C for 20 s, and extension at 72 °C for 20 s. Fluorescence signal was monitored at 585 nm during each extension. Glyceraldehyde 3-phosphate dehydrogenase (GAPDH) served as an internal control. Primers used in qRT-PCR are shown in Table 1.

Western Blot Analysis

Polyclonal rabbit antibodies for rat TGF-β1, Smad3, p-Smad3, ZEB1, ZEB2, Snail, Twist, and HMGA2 were purchased from Santa Cruz Biotechnology. HRP-labeled goat anti-rabbit IgG and α-tubulin antibody were from Beijing Zhong Shan-Golden Bridge Technology (Beijing, China). Total protein lysate samples containing 20 μg protein were subjected to 10% sodium dodecyl sulfate polyacrylamide gel electrophoresis, transferred onto polyvinylidene difluoride membranes, and blocked with 7% non-fat milk in Tris-buffered saline and Tween-20 (TBST; 50 mM Tris-HCl (pH 7.6),

Table 1 Primers of TGF-β1, Smad3, ZEB1, ZEB2, HMGA2, and GAPDH

Primer	Sequence
TGF-β1 sense	5′-CTACTACGCCAAAGAAGTCACC-3′
TGF-β1 antisense	5′-GAAAGCCCTGTATTCCGTCTC-3′
Smad3 sense	5′-TGTCATCTACTGCCGCTTGTG-3′
Smad3 antisense	5′-CAACACTGGAGGTAGCACTGG-3′
ZEB1 sense	5′-CCAAAGCAACAGGGAGAGTTAC-3′
ZEB1 antisense	5′-CTTGTCTTTCATCCTGGTTTCC-3′
ZEB2 sense	5′-TGATTGAGAACCACAGCATACC-3′
ZEB2 antisense	5′-GTTCATCAGAGTTGGGTTCCAT-3′
HMGA2 sense	5′-TGGTTGCTAATGAAGAGCCCG-3′
HMGA2 antisense	5′-CCAGATGAAAGTGGAAAGACC-3′
GAPDH sense	5′-GCACCGTCAAGGCTGAGAAC-3′
GAPDH antisense	5′-TGGTGAAGACGCCAGTGGA-3′

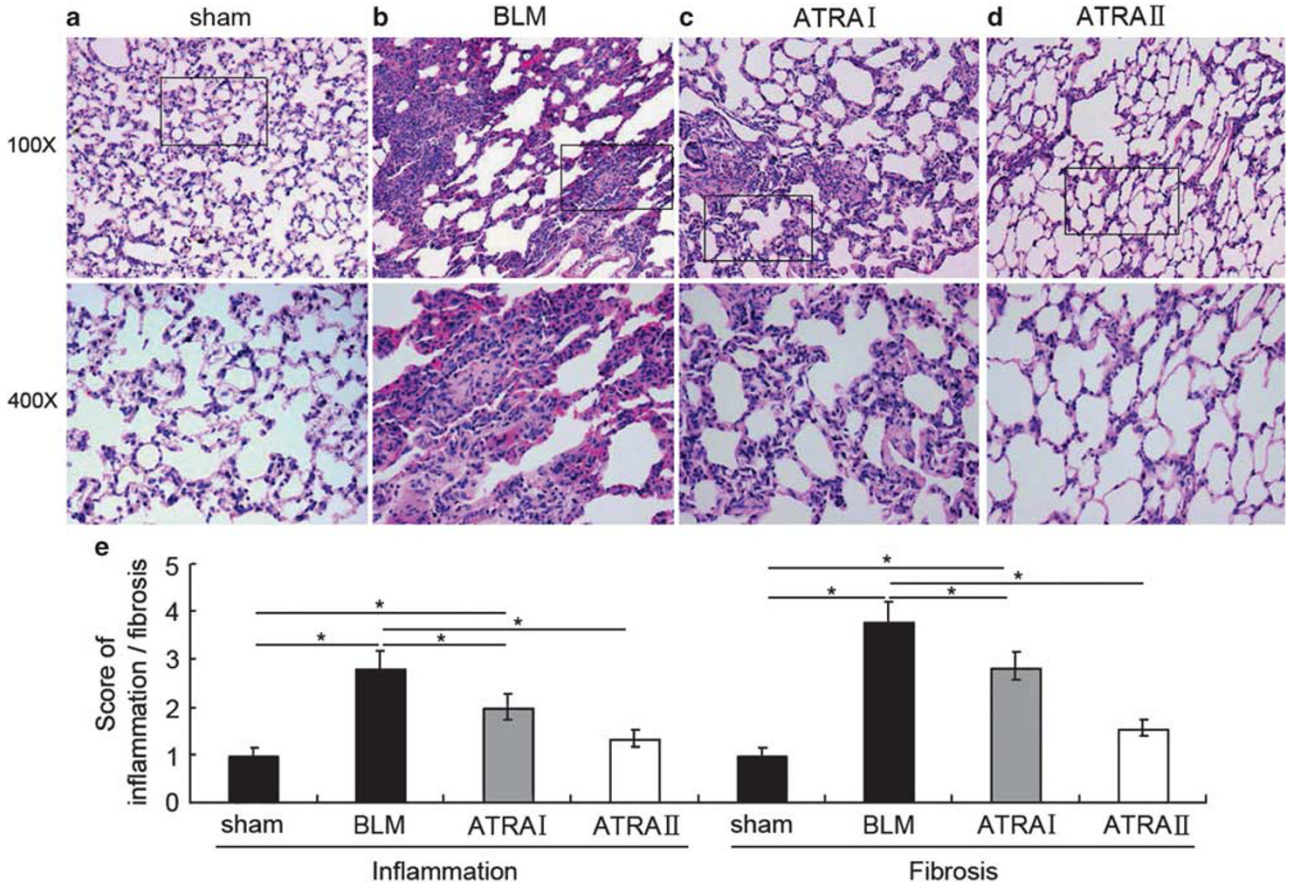

Figure 1 Grade of lung fibrosis and inflammation. (**a**) Sham group, (**b**) BLM group, (**c**) ATRA I group, (**d**) ATRA II group, and (**e**) score of lung fibrosis. Each bar represents the mean ± s.d., $n = 6$. Original magnification, × 400. *$P < 0.05$.

150 mM NaCl, 0.1% Tween-20) for 1.5 h at room temperature. Membranes were washed three times with TBST buffer and incubated at 4 °C overnight with polyclonal rabbit antibodies specific for rat TGF-β1, Smad3, p-Smad3, ZEB1, ZEB2, Snail, Twist, and HMGA2. After washing with TBST, membranes were incubated with HRP-labeled goat anti-rabbit IgG (1:5000) for 1.5 h at room temperature. Membranes were then washed with TBST, incubated with ECL reagent, and exposed. Membranes were subsequently stripped and re-probed with α-tubulin antibody (1:500), which served as loading control.

Statistical Analysis

Data are expressed as the mean ± s.e.m. of the indicated number of independent experiments. Student's *t*-test and one-way analysis of variance were used to determine significance, with $P < 0.05$ considered significant. The Kaplan–Meier method was used for survival analysis with a log-rank of $P < 0.05$ to determine significance. Statistical analyses were performed using SPSS 10.0 for Macintosh. Graphs were also constructed.

RESULTS

ATRA Prevented BLM-induced Lung Fibrosis

We first examined the preventive effect of ATRA on lung fibrosis by means of H&E staining, Masson's trichrome staining, immunohistochemistry, TEM, and Hyp content.

H&E staining results showed that tissue sections from the sham group had a continuous structure with an intact wall of bronchial mucous membrane and lung alveoli with no obvious abnormality. The alveoli in the sham group had clear hollow cavities with alveolar walls thinner than those in all other groups. The BLM group had the thickest alveolar walls among all the groups. Tissue sections from the BLM group also showed severe edema and infiltration of macrophages, neutrophils, lymphocytes, fibroblasts, and erythrocytes. In addition, the lung mesenchyme in the BLM group showed strong immunohistochemical staining for collagens and collagen fibers, indicating that the hallmark of the fibroblastic foci was distinctly present. These histological, cellular, and molecular characteristics of lung fibrosis were significantly reduced in ATRA-treated groups. Compared with the BLM group, tissue sections from ATRA-treated groups had thinner alveolar walls and showed lower degree of edema and cellular

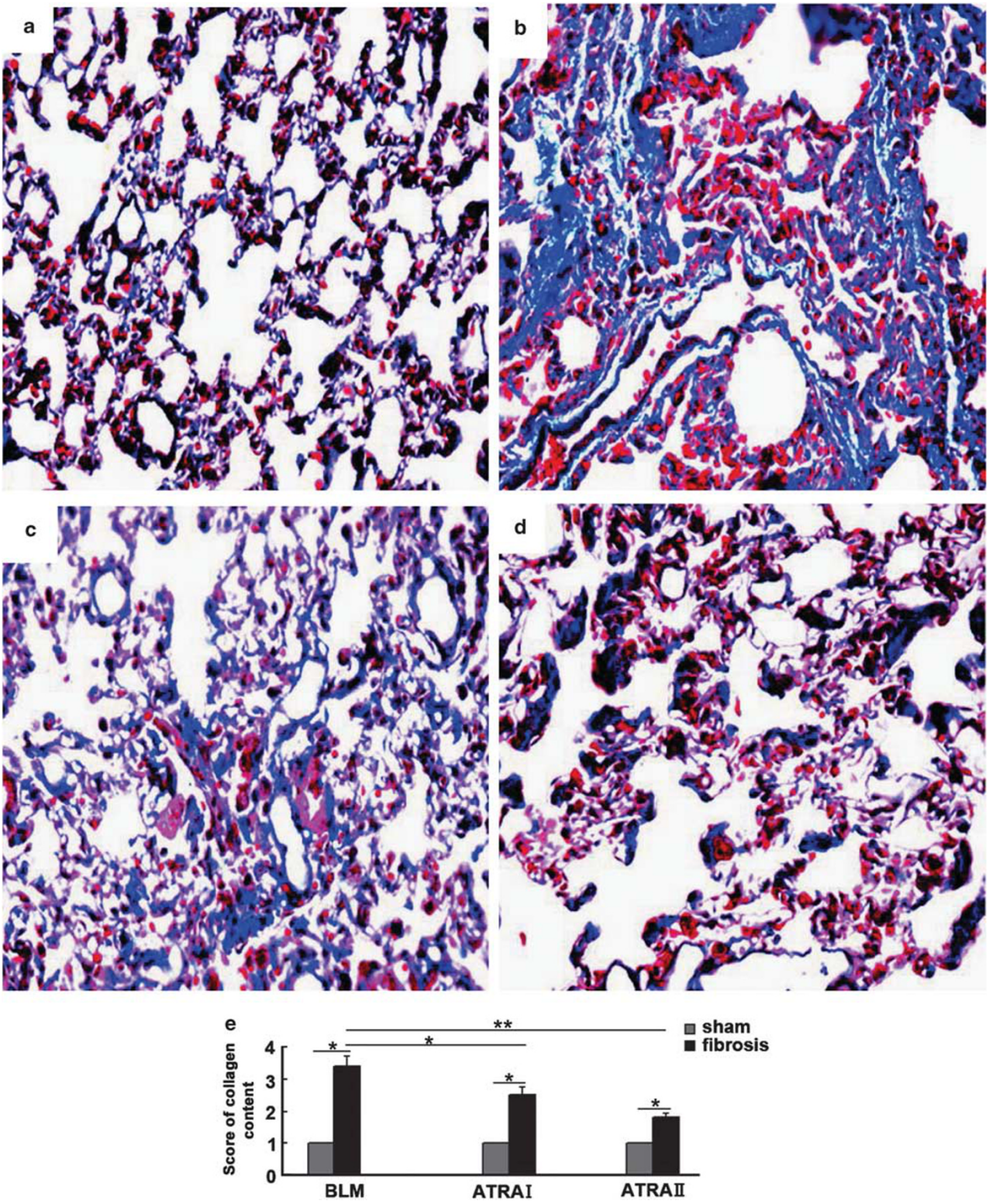

Figure 2 Collagen content (blue) observed with Masson's trichrome stain. (**a**) Sham group, (**b**) BLM group, (**c**) ATRA I group, (**d**) ATRA II group, and (**e**) score of collagen content. Each bar represents the mean ± s.d., $n = 6$. Original magnification, × 400. *$P < 0.05$; **$P < 0.01$.

infiltration of macrophages, neutrophils, lymphocytes, fibroblasts, and erythrocytes. Lung fibrosis determined by the Szapiel method using H&E staining showed statistically significant differences between ATRA-treated groups and the BLM group (Figure 1). Masson's trichrome staining showed that the number of fibroblasts and the collagen

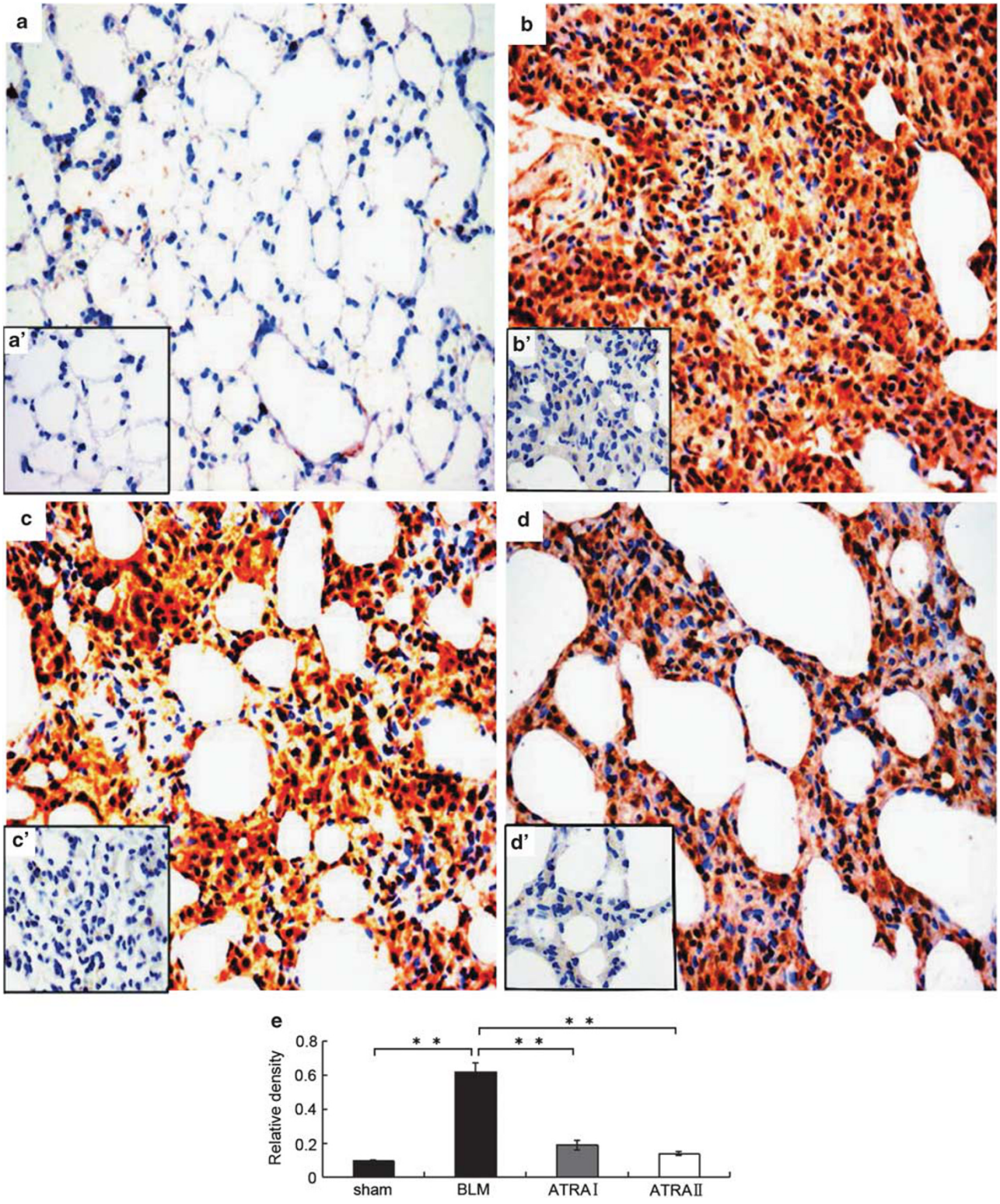

Figure 3 ATRA suppressed collagen I (brown) expression. (**a**) Sham group, (**b**) BLM group, (**c**) ATRA I group, (**d**) ATRA II group, (**e**) densitometric analyses, (a', b', c', d') negative control. Each bar represents the mean ± s.d., $n = 6$. Original magnification, × 400. $^{**}P < 0.01$.

matrix increased significantly in the BLM group, which was accompanied by formation of fibrosis lesions with cord-like distribution. ATRA treatment significantly reduced BLM-induced alveolitis and lung fibrosis (Figure 2). Immunohistochemical analysis indicated that the BLM group had higher collagen I content compared with the sham

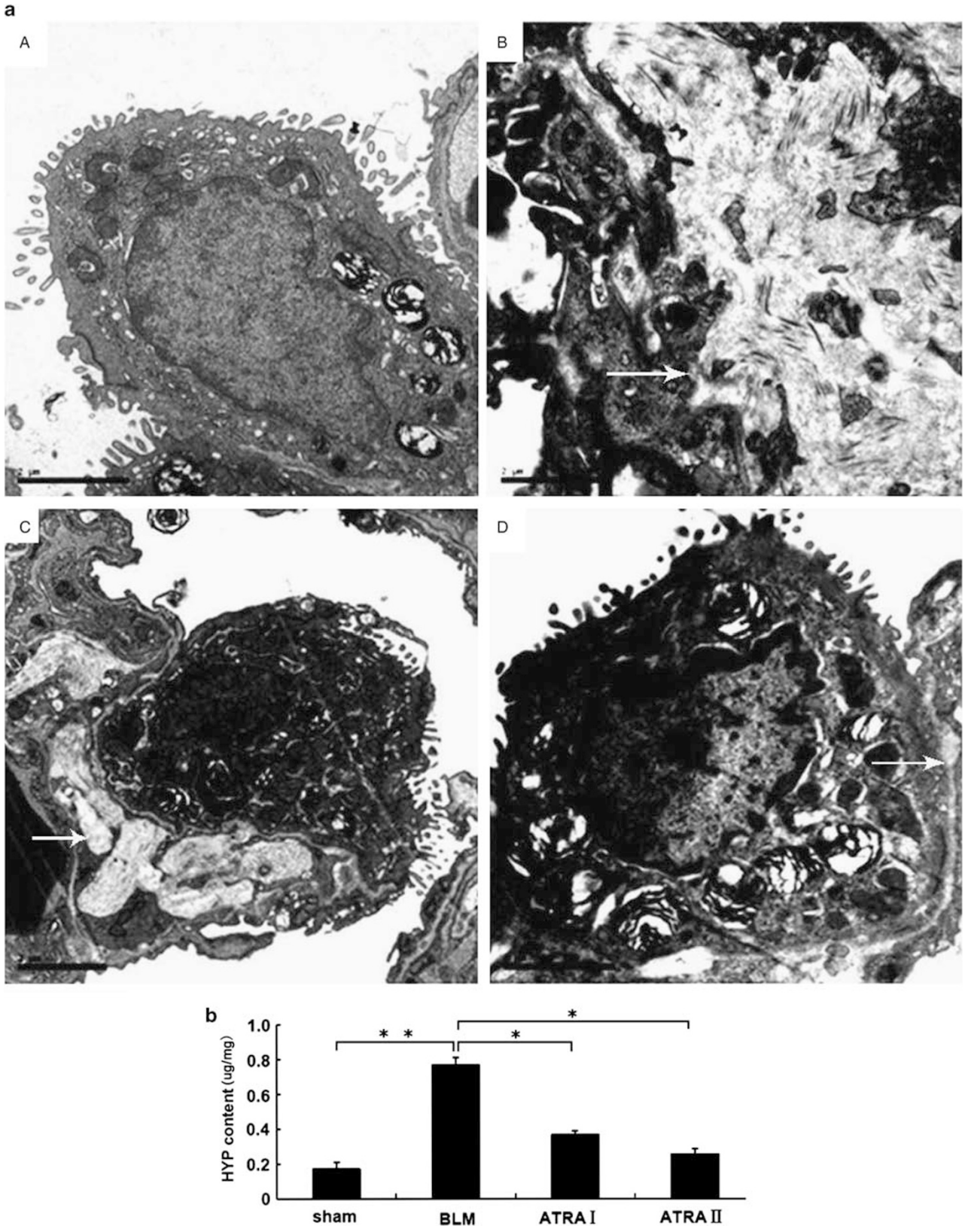

Figure 4 ATRA suppressed formation of collagen fibers and collagen deposition. (**a**) Collagen fibers (white arrow) observed under TEM. (A) The sham group exhibited the lowest number of collagen fibers in the interstitial lung tissue. (B) The BLM group showed the highest number of collagen fibers in the interstitial lung tissue. (C) ATRA I and (D) ATRA II groups exhibited significantly reduced collagen fibers. (**b**) Hyp content. Each bar represents the mean ± s.d., $n = 6$. $^{*}P < 0.05$, $^{**}P < 0.01$.

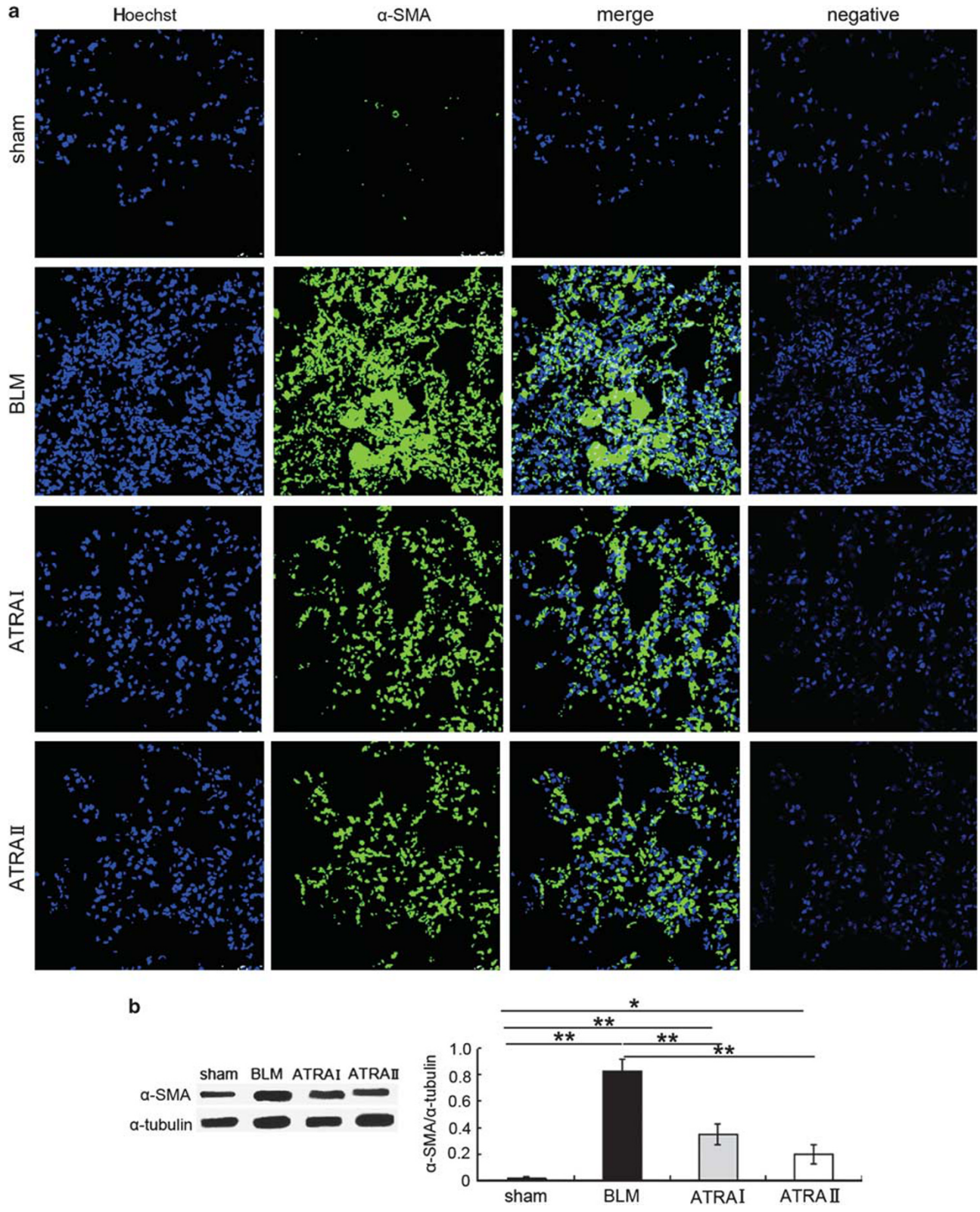

Figure 5 ATRA treatment suppressed α-SMA expression. (**a**) α-SMA expression (green) observed under a laser scanning confocal microscope. Nuclei (blue) were counterstained with hoechst 33342. (**b**) western blot analysis of α-SMA protein expression with densitometric quantification. Each bar represents the mean ± s.d., $n = 6$. *$P < 0.05$, **$P < 0.01$.

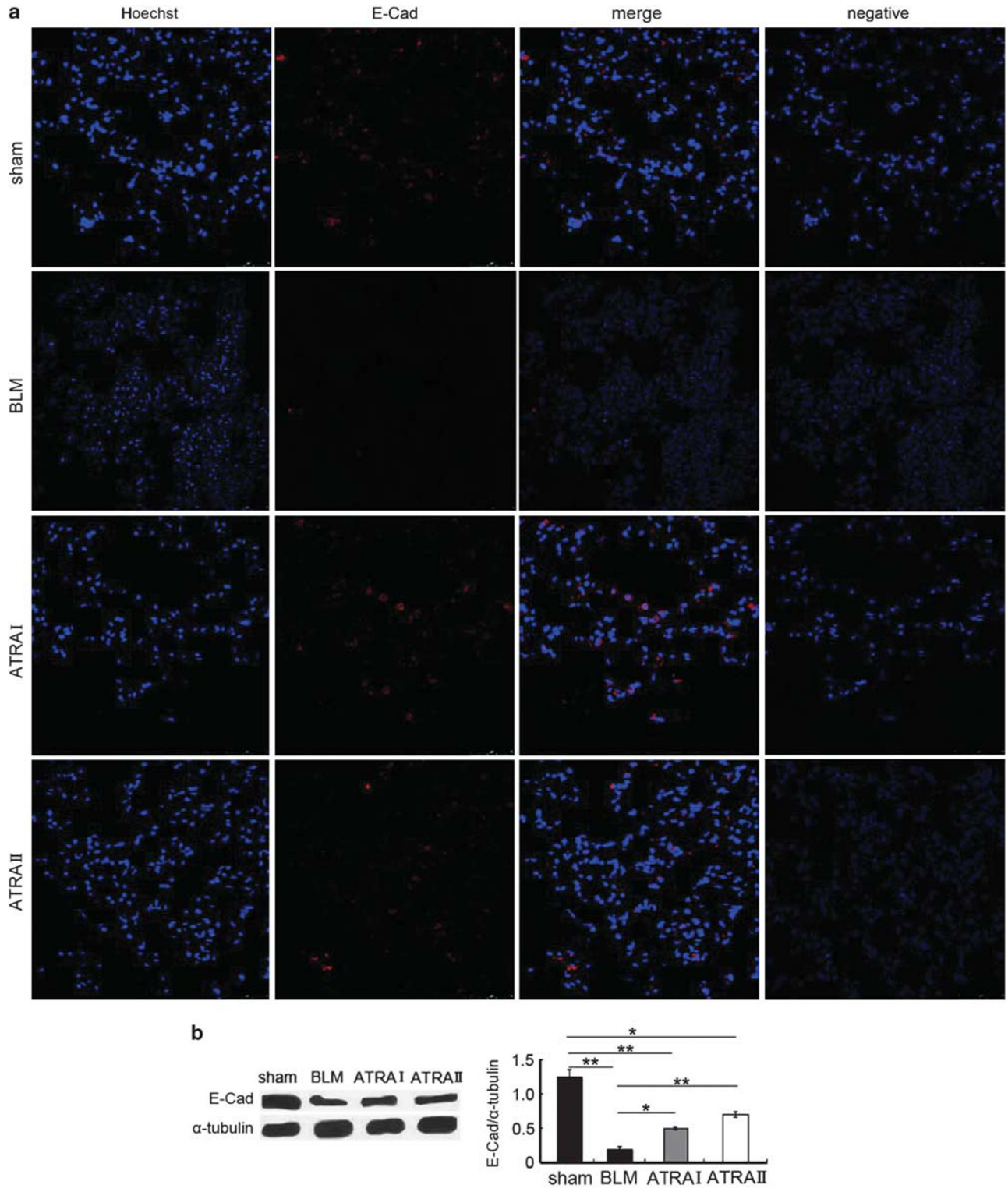

Figure 6 ATRA treatment increased E-cadherin expression. (**a**) E-cadherin expression (red) observed under a laser scanning confocal microscope. Nuclei (blue) were counterstained with hoechst 33342. (**b**) Western blot analysis of E-cadherin protein expression with densitometric quantification. Each bar represents the mean ± s.d., $n = 6$. *$P < 0.05$, **$P < 0.01$.

group, and ATRA treatment significantly attenuated BLM-induced collagen I expression (Figure 3). TEM results indicated that the sham group had the lowest number of collagen fibers among all the groups. The BLM group had a large number of collagen fibers in the interstitial lung and ATRA treatment significantly reduced BLM-induced formation of

collagen fibers (Figure 4a). Collagen deposition in the lung was assessed by Hyp content. Compared with the sham group, the BLM group showed significantly higher Hyp content in the lung. ATRA treatment significantly reduced BLM-induced increase in Hyp content (Figure 4b). In general, ATRA improved histological, cellular, and molecular markers of lung fibrosis in a dose-dependent manner.

ATRA Reduced Expression of EMT Markers

EMT is characterized by expression of the mesenchymal marker α-SMA and loss of the epithelial cell marker E-cadherin. Several transcription repressors such as Snail and Twist are involved in EMT. Immunofluorescence imaging and western blot analysis were used to analyze the expression of α-SMA, E-cadherin, Snail, and Twist. The immunofluorescence data showed that α-SMA level was significantly higher (Figure 5), whereas E-cadherin level was significantly lower (Figure 6) in the BLM group compared with the sham group. ATRA treatment markedly blocked BLM-induced changes in α-SMA and E-cadherin expression. Western blot analysis showed similar effects of BLM and ARTA on α-SMA and E-cadherin expression as those observed in immunofluorescence. In addition, ARTA downregulated BLM-induced Snail and Twist expression with kinetics similar to that observed with α-SMA (Figure 7).

ATRA Downregulated the TGF-β1/Smad3 Signaling Pathway

The effects of ATRA on the activation of the TGF-β1/Smad3 signaling pathway, including TGF-β1, Smad3, p-Smad3, and ZEB1, ZEB2, and HMGA2 regulated by the TGF-β1/Smad3 signaling pathway were assessed using qRT-PCR and western blot analyses. The qRT-PCR analysis showed that ATRA significantly reduced mRNA expression of these proteins in a concentration-dependent manner compared with the BLM group (Figures 8 and 9). Analysis of protein expression using western blot indicated similar effects of BLM and ATRA on the TGF-β1/Smad3 signaling pathway at the protein level (Figures 10 and 11).

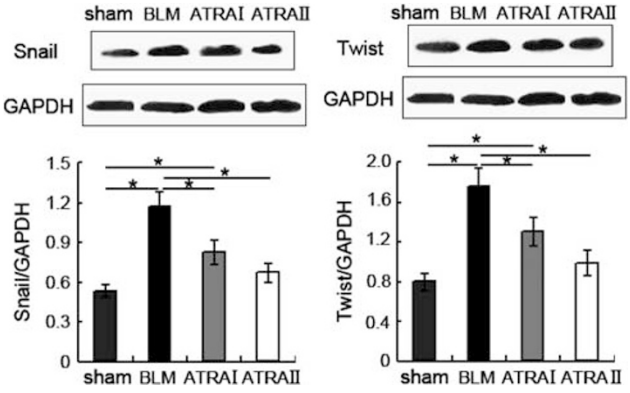

Figure 7 Western blot analysis of Snail and Twist protein expression with densitometric quantification. Each bar represents the mean ± s.d., $n = 6$. $^{*}P < 0.05$.

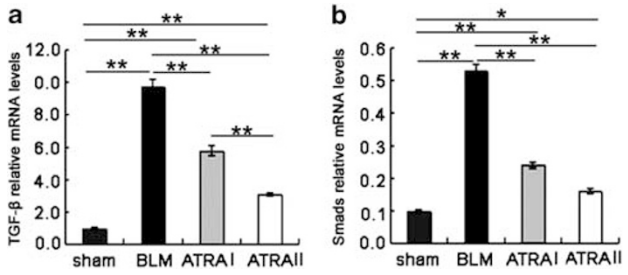

Figure 8 qRT-PCR analysis of TGF-β1 (**a**) and Smad3 (**b**) mRNA expression. Each bar represents the mean ± s.d., $n = 6$. $^{*}P < 0.05$, $^{**}P < 0.01$.

DISCUSSION

In the present study, we investigated the effect of ATRA on BLM-induced lung fibrogenesis in rats and the role of TGF-β1/Smad3 signaling pathway in ATRA treatment. Our results showed that BLM significantly increased alveolar wall thickness, inflammatory cell infiltration, and collagen fiber formation. These BLM-induced changes were significantly ameliorated by ATRA treatment, and these anti-fibrotic effects of ATRA may be mediated by EMT inhibition through the downregulation of the TGF-β1/Smad3 signaling pathway.

Our data showed that ATRA ameliorated BLM-induced EMT by inhibiting α-SMA and collagen expression and by enhancing E-cadherin expression in fibroblasts. These data are in agreement with the notion that fibroblasts are the primary effectors of tissue fibrosis because fibroblasts produce collagen and other extracellular matrix proteins.[24] In lung fibrogenesis, fibroblasts often differentiate into myofibroblasts, which exhibit enhanced fibrotic, contractile, and migratory activities.[25] α-SMA is a marker of myofibroblasts and a primary contributor to the contractile force in myofibroblasts.[26] It is believed that lung tissue fibrosis is regulated by the TGF-β1/Smad3 signaling pathway, which is activated by myofibroblast contraction.[27–31] The TGF-β1/Smad3 signaling pathway promotes fibrotic transformation of lung tissues via activation of EMT.[32–34]

EMT is a process in which epithelial cells lose their epithelial phenotype, acquire fibroblast-like properties, and display reduced cell adhesion and increased motility. Reduction in expression of adhesion molecules allows the cells to detach from the epithelial layer and migrate towards the site of injury or inflammation where they exercise their profibrotic effects. EMT has attracted considerable attention from researchers in the past few years as a potential contributor to fibrotic diseases.[35–37] Previous studies have demonstrated that epithelial cells undergoing EMT have decreased levels of epithelial cell markers such as E-cadherin and increased levels of myofibroblast markers such as α-SMA and mesenchymal cell marker collagen.[38,39]Our data that ATRA inhibited α-SMA and collagen expression and

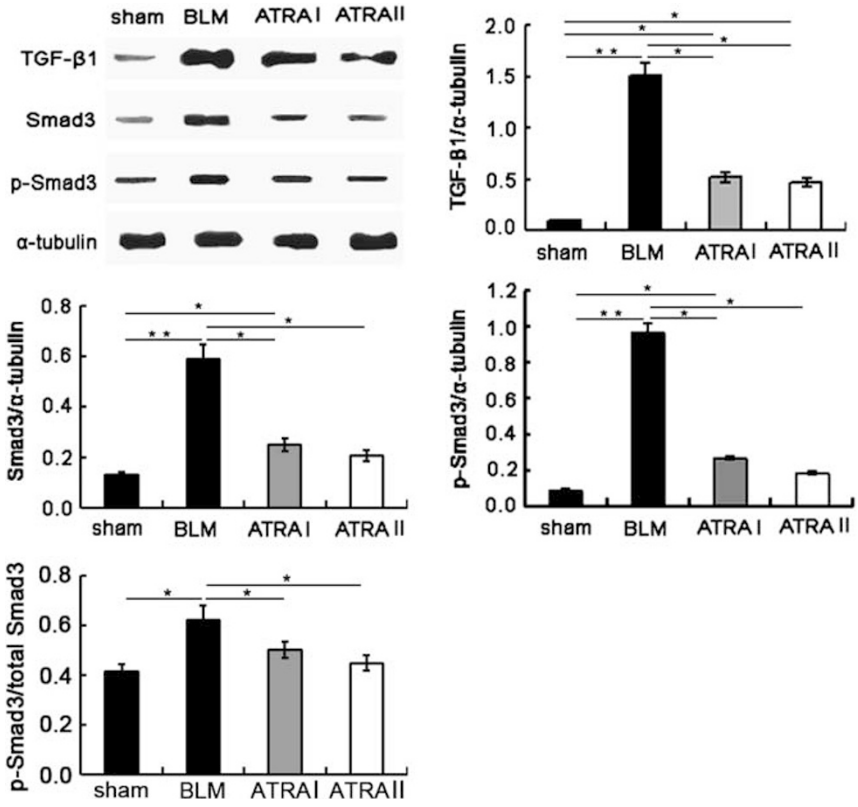

Figure 9 Western blot analysis of TGF-β1 and Smad3 protein expression with densitometric quantification. Each bar represents the mean ± s.d., $n = 6$. $^{*}P < 0.05$, $^{**}P < 0.01$.

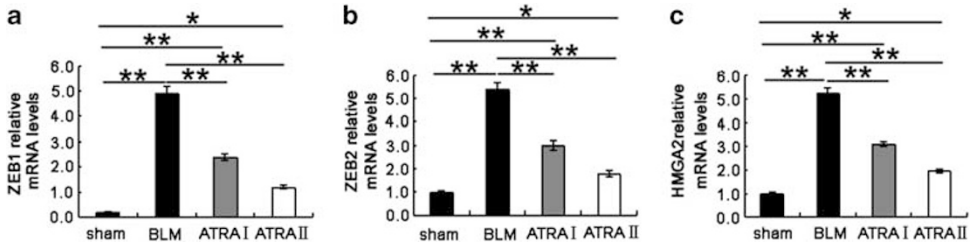

Figure 10 qRT-PCR analysis of ZEB1 (**a**), ZEB2 (**b**), and HMGA2 (**c**) mRNA expression. Each bar represents the mean ± s.d., $n = 6$. $^{*}P < 0.05$, $^{**}P < 0.01$.

increased the E-cadherin level support that ATRA might ameliorate lung fibrosis via suppressing EMT. To further study the effect of ATRA on EMT, we examined the expression of Snail and Twist, two most thoroughly studied transcription factors involved in EMT.[40,41] It is believed that Snail directly inhibits E-cadherin, whereas Twist suppresses the expression of E-cadherin indirectly.[42] Gene overexpression studies have shown that Snail is sufficient to induce EMT, and snail deficiency attenuates TGF-β1-induced EMT in alveolar epithelial type II (ATII) cells.[43] Snail is also highly expressed in hyperplasic ATII cells in lung tissues from patients with IPF, supporting its role in the pathogenesis of IPF. Twist is a well-established master transcription regulator of EMT during embryogenesis and metastasis.[44] The abundant expression of Twist in alveolar epithelial cells is likely to contribute to EMT, which is an important source of fibroblasts in lung fibrosis. It has been reported that Snail and Twist are upregulated by TGF-β1 signaling. Consistent with its activation of E-cadherin expression, ATRA inhibited BLM-induced Snail and Twist expression, further supporting that ATRA ameliorated lung fibrosis via inhibiting EMT. Recent studies[40,43,45–47] support our findings. For example, Snail and Twist are upregulated by the majority of EMT inducers and they play a crucial role in this transforming event. Snail overexpression induces EMT and renal fibrosis *in vivo* in a mouse model. Snail expression is increased in human lung fibrosis and is essential to the control of TGF-β1-induced EMT in alveolar epithelial cells *in vitro*. Twist is reportedly involved in the cadherin switch as an inducer of N-cadherin expression.

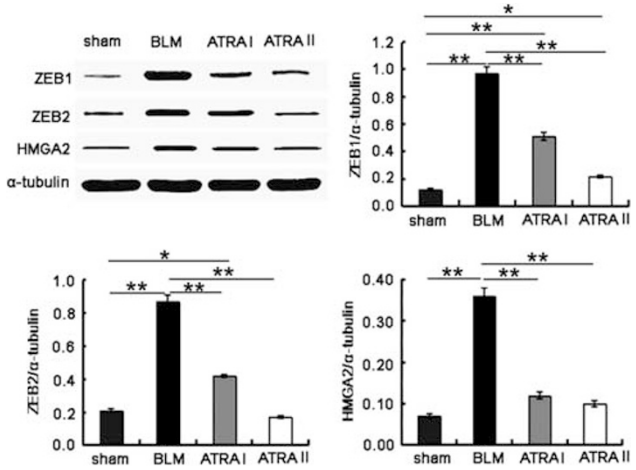

Figure 11 Western blot analysis of ZEB1, ZEB2, and HMGA2 protein expression with densitometric quantification. Each bar represents the mean ± s.d., $n = 6$. *$P < 0.05$, **$P < 0.01$.

HMGA2, ZEB1, and ZEB2 are transcription factors that promote EMT and are induced by the TGF-β1/Smad3 signaling pathway during the EMT process. HMGA2 upregulates the transcription of Snail and Twist, two transcriptional repressors of adherens that are critical for intercellular adhesions.[48,49] ZEB1 and ZEB2 are E-cadherin transcriptional repressors implicated in the initial stage of EMT.[50–52] ZEB1 and ZEB2 are upregulated during the pathogenesis of EMT. Xiong *et al*[53] demonstrated that the miR-200 family is responsible for protecting tubular EMT through the targeted suppression of ZEB1 and ZEB2. Ectopic expression of HMGA2, ZEB1, and ZEB2 cause irreversible EMT characterized by severe E-cadherin suppression and α-SMA enhancement.[54–58] Our results showed that BLM activated the TGF-β1/Smad3 signaling pathway including the expression of TGF-β1, Smad3, p-Smad3 and downstream effectors, and EMT promoters HMGA2, ZEB1, and ZEB2. ATRA blocked BLM-induced activation of the TGF-β1/Smad3 signaling pathway as shown in its inhibition of the expression of all these proteins.

In molecular terms, EMT tends to be induced by the Snail, Twist, and ZEB families of transcription factors, which may consequently be activated by the TGF-β1/Smad3 signaling pathway.[59] Taken together, our study provided the first line of evidence supporting the notion that ATRA can attenuate BLM-induced lung fibrosis by suppressing EMT. The inhibitory effect of ATRA on EMT is mediated by the downregulation of the TGF-β1/Smad3 signaling pathway. Further studies are needed to fully understand the mechanisms of ATRA action and exploit ATRA as a potential therapy for lung fibrosis.

ACKNOWLEDGEMENTS

This work was supported by grants from Taishan scholar position, Natural Science Foundation of China (NO. 81273957), Important Project of Science and Technology of Shandong Province (NO. 2010GWZ20254, NO. 2011GHY11501), Natural Science Foundation of Shandong Province (NO. ZR2009EM006, ZR2012HQ042), Project of Science and Technology of Education Department of Shandong Province (NO. J11FL87).

DISCLOSURE/CONFLICT OF INTEREST

The authors declare no conflict of interest.

1. du Bois RM. Strategies for treating idiopathic lung fibrosis. Nat Rev Drug Discov 2010;9:129–140.
2. Yang S, Cui H, Xie N, *et al.* miR-145 regulates myofibroblast differentiation and lung fibrosis. FASEB J 2013;27:2382–2391.
3. Zolak JS, Jagirdar R, Surolia R, *et al.* Pleural mesothelial cell differentiation and invasion in fibrogenic lung injury. Am J Pathol 2013;182:1239–1247.
4. Liu G, Friggeri A, Yang YP, *et al.* miR-21 mediates fibrogenic activation of lung fibroblasts and lung fibrosis. J Exp Med 2010;207:1589–1597.
5. Flanders KC. Smad3 as a mediator of the fibrotic response. Int J Exp Pathol 2004;85:47–64.
6. Zhao J, Shi W, Wang YL, *et al.* Smad3 deficiency attenuates bleomycininduced lung fibrosis in mice. Am J Physiol Lung Cell Mol Physiol 2002;282:585–593.
7. Dong XS, Hu XB, Liu W, *et al.* Effects of RNA interference-induced Smad3 gene silencing on lung fibrosis caused by paraquat in mice. Exp Biol Med 2012;237:548–555.
8. Xiao J, Meng XM, Huang XR, *et al.* miR-29 inhibits bleomycin-induced lung fibrosis in mice. Mol Ther 2012;20:1251–1260.
9. D'Alessandro-Gabazza CN, Kobayashi T, Boveda-Ruiz D, *et al.* Development and preclinical efficacy of novel transforming growth factor-β1 short interfering RNAs for lung fibrosis. Am J Respir Cell Mol Biol 2012;46:397–406.
10. Hamasaki T, Suzuki H, Shirohzu H, *et al.* Efficacy of a novel class of RNA interference therapeutic agents. PloS One 2012;7:e42655.
11. Eldman DR, Patil S, Trinos MJ, *et al.* Progression-free and overall survival in patients with relapsed/refractory germ cell tumors treated with single-agent chemotherapy: endpoints for clinical trial design. Cancer 2012;118:981–986.
12. Guo P, Chen HJ, Wang QY, *et al.* Down regulation of N-acetylglucosaminyltransferase V facilitates all-transretinoic acid to induce apoptosis of human hepatocarcinoma cells. Mol Cell Biochem 2006;284: 103–110.
13. Chiharu T, Yoshio K, Rie T, *et al.* All-trans-retinoic acid prevents radiation- or bleomycin-induced lung fibrosis. Am J Respir Crit Care Med 2006;174, 1352–1360.
14. Dong ZX, Tai WL, Yang YN, *et al.* The role of all-trans retinoic acid in bleomycin-induced lung fibrosis in mice. Exp Lung Res 2012;38: 82–89.
15. Segel MJ, Or R, Tzurel A, *et al.* All-trans-retinoic acid (ATRA) is of no benefit in bleomycin-induced lung injury. Pulm Pharmacol Ther 2001;14:403–407.
16. Li ZY, Zhou TB, Qin YH, *et al.* All-Trans retinoic acid attenuates the renal interstitial fibrosis lesion in rats but not by transforming growth factor-β1/Smad3 signaling pathway. Ren Fail 2013;35:262–267.
17. Zhou TB, Drummen GP, Qin YH. The controversial role of retinoic Acid in fibrotic diseases: analysis of involved signaling pathways. Int J Mol Sci 2012;14:226–243.
18. Wang MR, Zhang JJ, Song XD, *et al.* Astaxanthin ameliorates lung fibrosis in vivo and in vitro by preventing transdifferentiation, inhibiting proliferation, and promoting apoptosis of activated cells. Food Chem Toxicol 2013;56:450–458.
19. Saadeddin A, Torres-Molina F, Cárcel-Trullols J, *et al.* Pharmacokinetics of the time-dependent elimination of all-trans-retinoic acid in rats. AAPS Pharm Sci 2004;6:1–9.
20. Szapiel SV, Elson NA, Fulmer JD, *et al.* Bleomycin-induced interstitial pulmonary disease in the nude, athymic mouse. Am Rev Respir Dis 1979;120:893–899.
21. Loughlin PM, Cooke TG, George WD, *et al.* Quantifying tumour-infiltrating lymphocyte subsets: a practical immuno-histochemical method. J Immunol Methods 2007;321:32–40.
22. Song XD, Zhang JJ, Wang MR, *et al.* Astaxanthin induces mitochondria-mediated apoptosis in rat hepatocellular carcinoma CBRH-7919 cells. Biol Pharm Bull 2011;34:839–844.

23. Cao GH, Zhang JJ, Wang MR, *et al.* Differential expression of long non-coding RNAs in bleomycin-induced lung fibrosis. Int J Mol Med 2013;32:355–364.
24. Hardie WD, Glasser SW, Hagood JS. Emerging concepts in the pathogenesis of lung fibrosis. Am J Pathol 2009;175:3–16.
25. Tomasek JJ, Gabbiani G, Hinz B, *et al.* Myofibroblasts and mechano-regulation of connective tissue remodelling. Nat Rev Mol Cell Biol 2002;3:349–363.
26. Hinz B, Phan SH, Thannickal VJ, *et al.* Recent developments in myofibroblast biology: paradigms for connective tissue remodeling. Am J Pathol 2012;180:1340–1355.
27. Pottier N, Maurin T, Chevalier B, *et al.* Identification of keratinocyte growth factor as a target of microrna-155 in lung fibroblasts: implication in epithelial-mesenchymal interactions. PloS One 2009; 4:e6718.
28. Yu H, Konigshoff M, Jayachandran A, *et al.* Transgelin is a direct target of tgf-beta/smad3-dependent epithelial cell migration in lung fibrosis. FASEB J 2008;22:1778–1789.
29. Willis BC, Borok Z. Tgf-beta-induced emt: mechanisms and implications for fibrotic lung disease. Am J Physiol Lung Cell Mol Physiol 2007;293:L525–L534.
30. Brigham C, Willis ZB. TGF-β1-induced EMT: mechanisms and implications for fibrotic lung disease. Am J Physiol Lung Cell Mol Physiol 2007;293:L525–L534.
31. Jain M, Rivera S, Monclus EA, *et al.* Mitochondrial reactive oxygen species regulate TGF-beta signaling. J Biol Chem 2013;288:770–777.
32. Meng J, Zou YQ, Hu CP, *et al.* Fluorofenidone attenuates bleomycin-induced lung inflammation and fibrosis in mice via restoring caveolin 1 expression and inhibiting mitogen-activated protein kinase signaling pathway. SHOCK 2012;38:567–573.
33. Salem S, Harris T, Mok JSL, *et al.* Transforming growth factor-b impairs glucocorticoid activity in the A549 lung adenocarcinoma cell line. Br J Pharmacol 2012;166:2036–2048.
34. Payal K, Naik PD, Bozyk J, *et al.* Periostinpromotes fibrosis and predicts progression in patients with Idiopathic Lung Fibrosis. Am J Physiol Lung Cell Mol Physiol 2012;303:L1046–L1056.
35. Vincent Jordan N, Prat A, Abell AN, *et al.* SWI/SNF chromatin-remodeling factor Smarcd3/Baf60c controls EMT by inducing Wnt5a signaling. Mol Cell Biol 2013;33:3011–3025.
36. Aparicio LA, Abella V, Valladares M, *et al.* Posttranscriptional regulation by RNA-binding proteins during epithelial-to-mesenchymal transition. Cell Mol Life Sci 2013 (e-pub ahead of print).
37. Barriga EH, Maxwell PH, Reyes AE, *et al.* The hypoxia factor Hif-1α controls neural crest chemotaxis and epithelial to mesenchymal transition. J Cell Biol 2013;201:759–776.
38. Lekkerkerker AN, Aarbiou J, van Es T, *et al.* Cellular players in lung fibrosis. Curr Pharm Des 2012;18:4093–4102.
39. Milara J, Peiró T, Serrano A, *et al.* Epithelial to mesenchymal transition is increased in patients with COPD and induced by cigarette smoke. Thorax 2013;68:410–420.
40. Wettstein G, Bellaye PS, Kolb M, *et al.* Inhibition of HSP27 blocks fibrosis development and EMT features by promoting Snail degradation. FASEB J 2013;27:1549–1560.
41. Zheng H, Kang Y. Multilayer control of the EMT master regulators. Oncogene 2013; doi:10.1038/onc.2013.128.
42. Yang J, Weinberg RA. Epithelial-mesenchymal transition: at the crossroads of development and tumor metastasis. Dev Cell 2008;14: 818–829.
43. Jayachandran A, Konigshoff M, Yu H, *et al.* SNAI transcription factors mediate epithelial-mesenchymal transition in lung fibrosis. Thorax 2009;64:1053–1061.
44. Sharma AK, Hubmayr RD. Epithelial to mesenchymal transition: a new twist to biotrauma. Crit Care Med 2012;40:682–683.
45. Boutet A, De Frutos CA, Maxwell PH, *et al.* Snail activation disrupts tissue homeostasis and induces fibrosis in the adult kidney. EMBO J 2006;25:5603–5613.
46. Galván JA, Astudillo A, Vallina A, *et al.* Epithelial-mesenchymal transition markers in the differential diagnosis of gastroenteropancreatic neuroendocrine tumors. Am J Clin Pathol 2013;140:61–72.
47. Alexander NR, Tran NL, Rekapally H, *et al.* N-cadherin gene expression in prostate carcinoma is modulated by integrin-dependent nuclear translocation of Twist1. Cancer Res 2006;66:3365–3369.
48. Sylvie T, Ulrich V, Maj P, *et al.* Transforming growth factor-β employs HMGA2 to elicit epithelial–mesenchymal transition. J Cell Biol 2006;174:175–183.
49. Thuault S, Tan EJ, Peinado H, *et al.* HMGA2 and Smads co-regulate SNAIL1 expression during induction of epithelial-to-mesenchymal transition. J Biol Chem 2008;283:33437–33446.
50. Xiong M, Jiang L, Zhou Y, *et al.* The miR-200 family regulates TGF-_ 1-induced renal tubular epithelial to mesenchymal transition through Smad pathway by targeting ZEB1 and ZEB2 expression. Am J Physiol Renal Physiol 2012;302:F369–F379.
51. Korpal M, Lee ES, Hu G, *et al.* The miR-200 family inhibits epithelial-mesenchymal transition and cancer cell migration by direct targeting of E-cadherin transcriptional repressors ZEB1 and ZEB2. J Biol Chem 2008;283:14910–14914.
52. Park SM, Gaur AB, Lengyel E, *et al.* The miR-200 family determines the epithelial phenotype of cancer cells by targeting the E-cadherin repressors ZEB1 and ZEB2. Genes Dev 2008;22:894–907.
53. Xiong M, Jiang L, Zhou Y, *et al.* The miR-200 family regulates TGF-β1-induced renal tubular epithelial to mesenchymal transition through Smad pathway by targeting ZEB1 and ZEB2 expression. Am J Physiol Renal Physiol 2012;302:F369–F379.
54. Zhu C, Li J, Cheng G, *et al.* miR-154 inhibits EMT by targeting HMGA2 in prostate cancer cells. Mol Cell Biochem 2013;379:69–75, PMID: 23591597.
55. Tan EJ, Thuault S, Caja L, *et al.* Regulation of transcription factor Twist expression by the DNA architectural protein high mobility group A2 during epithelial-to-mesenchymal transition. J Biol Chem 2012;287: 7134–7145.
56. Kitase Y, Shuler CF. Microtubule disassembly prevents palatal fusion and alters regulation of the E-cadherin/catenin complex. Int J Dev Biol 2013;57:55–60.
57. Gheldof A, Berx G. Cadherins and epithelial-to-mesenchymal transition. Prog Mol Biol Transl Sci 2013;116:317–336.
58. Sánchez-Tilló E, Liu Y, de Barrios O, *et al.* EMT-activating transcription factors in cancer: beyond EMT and tumor invasiveness. Cell Mol Life Sci 2012;69:3429–3456.
59. Nieto MA. The ins and outs of the epithelial to mesenchymal transition in health and disease. Annu Rev Cell Dev Biol 2011;27:347–376.